



Results of Initial Alloy 617 High Temperature Crack Growth Testing

September 2022

Joseph Bass
Idaho National Laboratory



*INL is a U.S. Department of Energy National Laboratory
operated by Battelle Energy Alliance, LLC*

DISCLAIMER

This information was prepared as an account of work sponsored by an agency of the U.S. Government. Neither the U.S. Government nor any agency thereof, nor any of their employees, makes any warranty, expressed or implied, or assumes any legal liability or responsibility for the accuracy, completeness, or usefulness, of any information, apparatus, product, or process disclosed, or represents that its use would not infringe privately owned rights. References herein to any specific commercial product, process, or service by trade name, trade mark, manufacturer, or otherwise, does not necessarily constitute or imply its endorsement, recommendation, or favoring by the U.S. Government or any agency thereof. The views and opinions of authors expressed herein do not necessarily state or reflect those of the U.S. Government or any agency thereof.

Results of Initial Alloy 617 High Temperature Crack Growth Testing

**Joseph Bass
Idaho National Laboratory**

September 2022

**Idaho National Laboratory
Advanced Reactor Technologies
Idaho Falls, Idaho 83415**

<http://www.art.inl.gov>

**Prepared for the
U.S. Department of Energy
Office of Nuclear Energy
Under DOE Idaho Operations Office
Contract DE-AC07-05ID14517**

Page intentionally left blank

INL ART Program

Results of Initial Alloy 617 High Temperature Crack Growth Testing

INL/RPT-22-69322

Revision 0

September 2022

Technical Reviewer: (Confirmation of mathematical accuracy, and correctness of data and appropriateness of assumptions.)




Michael McMurtrey
INL ART high Temperature Metals Lead

9/22/2022

Date


Approved by:



Michael E. Davenport
ART Project Manager

9/22/2022


Date



Travis R. Mitchell
ART Program Manager

9/22/2022

Date



Michelle T. Sharp
INL Quality Assurance

9/22/2022

Date

ABSTRACT

Crack propagation data can provide valuable insights when performing a safety evaluation for a component. Alloy 617 is qualified in Section III, Division 5 of the ASME Boiler and Pressure Vessel Code (BPVC) for elevated-temperature nuclear service up to 950°C. Little is known, however, about subcritical crack-growth phenomena in Alloy 617. Previous crack-growth studies of Alloy 617 did not investigate temperatures across the range which is currently qualified in Section III, Division 5. High-temperature crack-growth testing in air and in reactor-grade helium can provide data for establishing the crack-growth correlations in support of an ASME BPVC Section XI high-temperature flaw evaluation Code Case. Idaho National Laboratory (INL) has previously performed crack-growth testing, but the equipment requires revitalization. This report provides the status of crack-growth testing in Alloy 617 at INL.

Page intentionally left blank

CONTENTS

ABSTRACT.....	iv
FIGURES.....	vi
TABLES	vi
ACRONYMS.....	viii
1. INTRODUCTION.....	1
1.1 Motivation.....	1
1.2 Previous Work.....	1
1.2.1 Material Characterization.....	1
1.2.2 Environmental Crack Growth	2
2. CRACK-GROWTH TESTING	2
2.1 Experimental Setup	3
2.2 Crack-Growth Validation.....	3
2.3 Crack-Growth Testing in Laboratory Air	6
3. SUMMARY AND FUTURE WORK.....	7
4. References	8
Appendix A INL drawing 765572 Rev. 2.....	10

FIGURES

Figure 1. Fractured surface of C(T) specimen 617-46-ORD and corresponding crack measurements used for validating DCPD crack lengths.....	4
Figure 2. Crack length <i>versus</i> time for validation test outlined in Table 3.	6

TABLES

Table 1. Alloy 617 chemical composition requirements and heat 314626 composition (in weight percent).	1
Table 2. Comparison of corrected DCPD crack lengths and optically measured crack lengths.	5
Table 3. Fatigue steps in validation test at 800°C in lab air.....	5
Table 4. Crack-growth rates comparing this work to previous work.....	6
Table 5. Initial laboratory-air fatigue test steps.	7

Page intentionally left blank

ACRONYMS

ASTM	American Society for Testing and Materials
ASME	American Society of Mechanical Engineers
BPVC	Boiler and Pressure Vessel Code
C(T)	compact tension
DCPD	direct current potential drop
INL	Idaho National Laboratory

Page intentionally left blank

Results of Initial Alloy 617 High Temperature Crack Growth Testing

1. INTRODUCTION

1.1 Motivation

Alloy 617 has presented itself as a promising material for many applications including elevated-temperature nuclear applications. Alloy 617 is qualified in Section III, Division 5 of the American Society of Mechanical Engineers (ASME) Boiler and Pressure Vessel Code (BPVC) code for the construction of elevated-temperature nuclear components. It is qualified for a maximum service life and temperature of 100,000 hours and 950°C, respectively [1]. Although Section III, Division 5 provides rules for construction, it does not consider post-construction analysis which ensures that a component remains functional and safe. This analysis is covered in Section XI, Division 2 of the ASME BPVC. Section XI covers rules for in-service inspection of nuclear power plant components, and Division 2 covers requirements for reliability and integrity management (RIM) programs for nuclear power plants [1].

In nuclear applications, fatigue loads may be present in components manufactured from Alloy 617. It is known that no component is perfect and minor flaws created during manufacturing exist. From a safety perspective, it is important to have a solid understanding of how subcritical flaws will grow as a result of fatigue loading. High-temperature crack-growth tests in air and in reactor-grade helium would provide data for establishing the crack-growth correlations in support of a ASME BPVC Section XI high-temperature flaw evaluation Code Case. It is of particular importance to investigate the effects of environment as it has been observed that when exposed to various environments Alloy 617 can carburize, decarburize, and generate a protective oxide. These all have the potential to influence the crack-growth rates imparted by fatigue loading.

1.2 Previous Work

1.2.1 Material Characterization

The Alloy 617 plate used in this work was produced by ThyssenKrupp Vereinigte Deutsche Metallwerke, heat 314626. The chemical composition of this heat is provided in Table 1. In the table, the top two rows are the chemical composition requirements for Alloy 617 as specified by the American Society for Testing and Materials (ASTM) B168-19, “Standard Specification for Nickel-Chromium-Iron Alloys (UNS N06600, N06601, N06603, N06690, N06693, N06025, N06045, and N06696) and Nickel-Chromium-Cobalt-Molybdenum Alloy (UNS N06617) Plate, Sheet, and Strip” [2]. The bottom row is the composition of heat 314626 [3]. This table shows that the plate used in this crack-growth testing is within the composition limits specified in the standard. The significant strengthening mechanisms in Alloy 617 are solid solution strengthening from Co and Mo as well as precipitation strengthening. The main precipitates which can result in strengthening in Alloy 617 are $M_{23}C_6$, M_6C , and various Ti containing precipitates.

Table 1. Alloy 617 chemical composition requirements and heat 314626 composition (in weight percent).

	Ni	Cr	Co	Mo	Fe	Mn	Al	C	Cu	Si	S	Ti	B
Min	44.5	20	10	8	-	-	.8	.05	-	-	-	-	-
Max	-	24	15	10	3	1	1.5	.15	.5	1	.015	.6	.006
Plate	54.1	22.2	11.6	8.6	1.6	.1	1.1	.05	.04	.1	<.002	.4	<.001

The average grain size of the plate was determined by the lineal intercept method to be 150 μm ; although, it is noted the microstructure is significantly heterogeneous. In some areas, carbide banding was observed along with stringers which ran parallel to the rolling direction of the plate. Outside of the region containing the carbides, only a few Ti(C,N) precipitates were observed [3]. In the crack-growth testing in previous work, the Alloy 617 plate was aged and carburized which changed the microstructure. In this work, the plate material will be in the solution-annealed condition.

1.2.2 Environmental Crack Growth

The prior study on the effect of environment on crack growth in Alloy 617 was performed at Idaho National Laboratory (INL) [3]. This study investigated the effects of multiple variables including: 1) material processing (aged, carburized, solution annealed), 2) temperature (650°C and 800°C), 3) environment (air and impure helium), and 4) fatigue loading (frequency and magnitude). In the previous work, fatigue loads with a constant maximum stress intensity, K , were applied during a test. The main findings were:

- 1) Aging Alloy 617 at 650°C for 5300 hours did not result in any significant effect on the crack-growth rate. Although, as expected based on the time-temperature-transformation diagram, γ' (Ni_3Al) precipitates as well as additional carbides were formed.
- 2) Carburization appeared to increase crack-growth rates compared to the solution-annealed material.
- 3) Initially, an increase in fatigue load frequency resulted in a decreased crack-growth rate. Although, at higher frequencies the crack-growth rate approached a constant. This time dependent behavior was attributed to oxidation effects at the crack tip.
- 4) Cracks in the fatigued specimens showed an intragranular pathway, while tests run at constant stress intensity (creep) showed intergranular cracking.
- 5) In general, the crack-growth rates were higher for testing conducted in laboratory air when compared to testing in impure helium. Although, this trend was not observed for testing conducted at 800°C at low frequency.

2. CRACK-GROWTH TESTING

The crack-growth testing in this work applies fatigue loads which have a constant maximum stress intensity. The load application follows a triangular wave form. In order to apply a constant maximum stress intensity, the instantaneous crack length needs to be determined because $K \propto \sigma a^{.5}$, where a is the crack length and σ is the stress. A direct current potential drop (DCPD) setup measures the instantaneous crack length in a specimen during testing by measuring the potential drop and using a correlation to compute the corresponding crack length. A more in-depth discussion of the math and theory behind the DCPD crack measurement system used in this work can be found in an Engineering Calculation and Analysis Report put together by Richard Wright [4].

One concern about using a constant maximum stress intensity is that if the crack growth is controlled by creep at the crack tip, then C^* would be a better parameter to use for testing. Based on the fatigue testing in previous work, it was observed that the crack pathway was intragranular. This is consistent with a cracking mechanism controlled by fatigue. The intragranular pathway was observed for all fatigue frequencies. When the stress intensity was held constant, and the crack-growth pathway was observed to be intergranular. This intergranular crack growth is indicative that creep is the primary mechanism driving the crack growth. Based on these previous findings, it is reasonable to assume that even at the elevated temperatures proposed in this work, the main crack-growth mechanism is likely caused by fatigue and therefore K is reasonable to test with.

2.1 Experimental Setup

Crack-growth testing utilizes a test frame, furnace, and DCPD system to apply constant stress intensities to compact tension, C(T), specimens. The furnace attached to the test frame has a maximum temperature of 1000 °C. The crack-growth testing follows the protocols in ASTM E 647-15. The C(T) specimens follow the requirements in Annex A1 of the standard. The specimens were machined from the Alloy 617 plate discussed in section 1.2.1 using INL Drawing 765572 Rev. 2. See Appendix A. A total of 24 C(T) specimens were machined, 12 of which have their notch machined parallel to the rolling direction, and 12 with their notch orthogonal to the rolling direction. It is not expected that the specimen's orientation with respect to the rolling direction will have a significant effect on the crack-growth rates, but this will allow for that aspect to be investigated.

As mentioned previously, while INL has performed crack-growth testing in the past, but the equipment was in need of revitalization. The setup to perform in-air testing is complete and functional. In FY23 the environmental control system will be setup on a second load frame so that crack-growth testing in environments other than laboratory air can be run. The other environment of interest in this work is impure helium which corresponds to the expected environment in a helium cooled reactor.

2.2 Crack-Growth Validation

The crack-growth experiments apply a fatigue load with a constant maximum stress intensity, K , to open a crack in the C(T) specimens. To validate that the experimental setup is functioning as intended, it is necessary to verify that the intended load is being applied. In order for the correct load to be applied, it must be confirmed that the DCPD is computing a crack length which matches the crack length in the specimen. The actual crack length can be determined post-test by imaging the fractured specimen and measuring the location of the crack at transitions in fatigue load. This is possible because when the fatigue load is changed, there is an identifiable change on the fractured surface of the specimen. Once it is confirmed that the DCPD accurately computes the crack length, it is possible to determine the actual stress intensity which is being applied.

A validation test to confirm the accuracy of the crack length computed by the DCPD was run on specimen 617-46-ORD at 800°C in air. The maximum stress intensity and frequency of the fatigue load were changed several times during the test. At the end of the test, a high load was applied to fully fracture the specimen. The fractured surface was imaged and measured post-test. The image of the fractured surface and crack measurements are shown in Figure 1. In the figure, the bottom white horizontal line is the initial crack tip which was created when the specimens were machined, and the color variation on the specimen surface shows the crack location at transition in fatigue load. In this test, there were five loads applied during the test. These different loads will be referred to as steps. In the figure, the transition from step 2 to step 3 is quite apparent as the color of the surface changes significantly, but the transition in the other steps is not as easily seen in the figure.

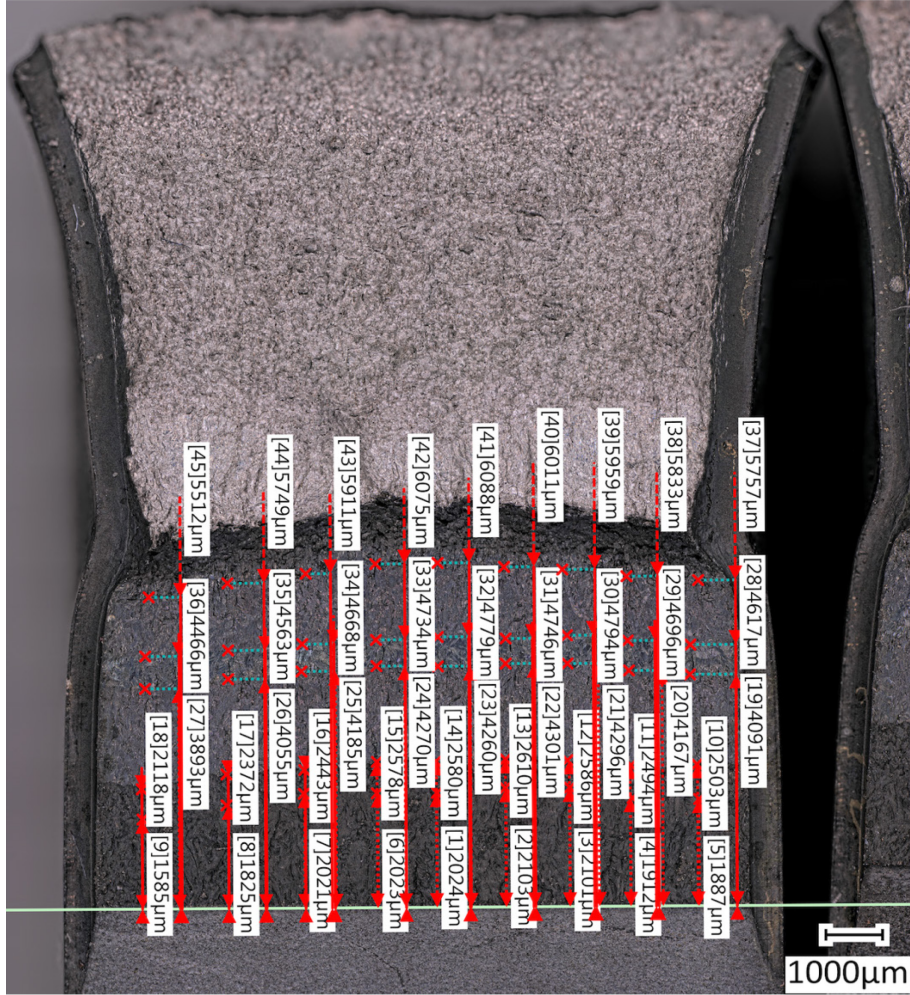


Figure 1. Fractured surface of C(T) specimen 617-46-ORD and corresponding crack measurements used for validating DCPD crack lengths.

It should also be noted that there are several measurements taken at each step transition in the figure. This is because the crack tip location varies slightly along the width of the specimen with the largest cracks generally occurring in the specimen center. The 'x' labels in Figure 1 mark the locations of some of the transitions in the fatigue loading steps and the large region at the top of the specimen is the portion of the specimen which was subjected to a large load in order to full fracture the specimen. As the DCPD only computes a single crack length value we need a single optically measured crack length for comparison. In the following analysis, the optically measured crack length at each transition is computed by averaging the measurements at that transition.

The output crack length from the DCPD undergoes a correction which adjusts the DCPD potential to recalibrate the output so that the first crack transition matches the end of the optically measured first crack location. This process is discussed in detail elsewhere [4]. Table 2 shows a comparison of the crack length divided by 'w' which is the distance between the applied load in the specimen to the end of the specimen. In the table 'Opt.' is the optically measured value. As can be seen from the table, after correction, the difference between the optically measured value and the value from the DCPD was less than three percent for the entirety of the validation test.

Table 2. Comparison of corrected DCPD crack lengths and optically measured crack lengths.

Step	Corrected DCPD measured a/w	Opt. measured a/w	Percent Difference (Opt. – DCPD)/Opt.
1	0.473	0.473	0
2	0.49265	0.494	0.27
3	0.55133	0.560	1.55
4	0.57088	0.580	1.57
5	0.60997	0.627	2.7

A second validation test was run using the steps outlined in Table 3 below. In this table, R is the ratio of the minimum over the maximum load, and f is the frequency at which the load was applied. This test was run in laboratory air at 800°C, and the fatigue loads were applied using triangular wave forms where the frequency corresponds to the time between peaks in the load. It should be noted that the loads in the table are the input loads. The true maximum stress intensity will vary slightly because the applied load is based on an uncorrected DCPD crack length. Although, this correction to the DCPD crack length does not typically make a substantial change, so the Kmax in the table is likely close to the true applied load.

Table 3. Fatigue steps in validation test at 800°C in lab air.

Step	Kmax (MPa√m)	R	f (Hz)
1	16	0.1	1
2	18	0.7	0.5
3	16	0.1	1
4	18	0.7	0.5
5	16	0.1	1

This validation test has several useful features beyond allowing for the verification of the accuracy of the DCPD crack measurement. By transitioning back and forth between loads we can confirm that changing loads mid test does not affect the computed crack-growth rate. In other words, as long as the crack-growth rate in steps 1,3 and 5 match each other and the rate in 2 and 4 match, it is reasonable to assume that the order that the loads are applied has little effect on the result. Therefore, it is reasonable to apply multiple loads to the same specimen with confidence that prior loads are not affecting later results. The corrected DCPD crack growth during the test is plotted in Figure 2. Lines were fit to each of the steps as shown in the figure. The crack-growth rates are the slope of the lines and these are shown in the legend in the plot. Comparing the slopes of steps 1,3 and 5, we see that there is not a significant change. This holds when comparing steps 2 to 4 which supports that multiple loads can be run on the same specimen without altering the results.

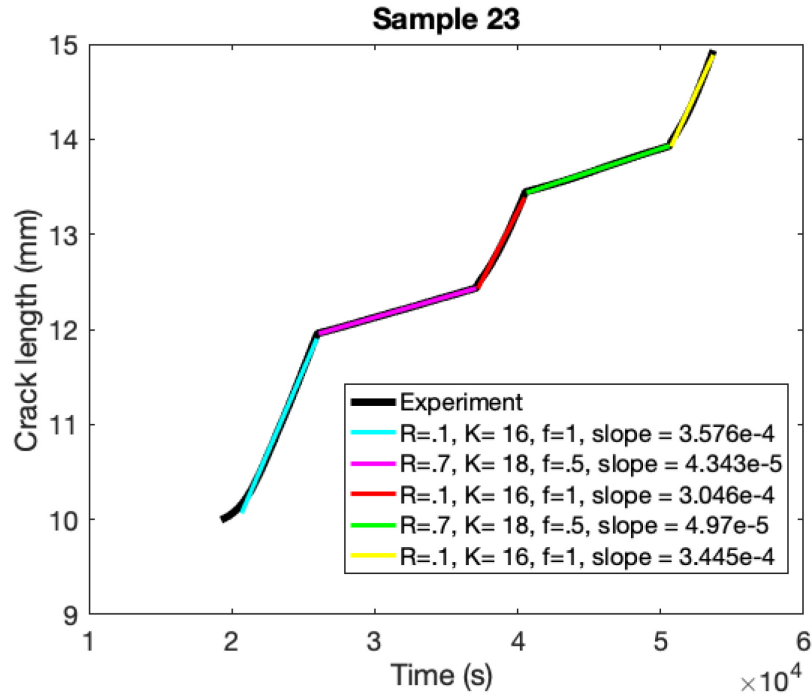


Figure 2. Crack length *versus* time for validation test outlined in Table 3.

It should be noted that in Figure 2, the slope during step 1 appears to be changing at the beginning and the fit line does not include this initial portion of the crack growth. This is because the machined notch in the specimen does not provide a true sharp crack tip which is an assumption of the experimental setup. A sharp crack tip is only produced after the crack has been extended by fatigue loading. That is why the initial portion of the slope is excluded from analysis.

The test in Table 3 used the same fatigue steps as a test conducted previously [4]. This allows for direct comparison of the computed crack-growth rates in this testing versus previous testing. Table 4 provides a comparison of the current results to the results from the previous work. It is seen that they match reasonably well with the current results showing a slightly faster crack-growth rate.

Table 4. Crack-growth rates comparing this work to previous work.

Step	Previous crack growth (mm/s) [4]	Current crack growth (mm/s)
1	3.195e-04	3.5767e-04
2	3.199e-05	4.3436e-05
3	2.195e-04	3.0466e-04
4	3.761e-05	4.9701e-05
5	2.537e-04	3.4448e-04

2.3 Crack-Growth Testing in Laboratory Air

The crack-growth testing in laboratory air will investigate temperatures Alloy 617 is qualified to in Section III, Division 5 of the ASME BPVC. Specifically, crack-growth correlations from fatigue loading will be investigated up to 1000°C. The first high-temperature, laboratory-air test will be at 900°C and have the loading steps shown in Table 5.

Table 5. Initial laboratory-air fatigue test steps.

Step number	K _{max} (MPa√ <i>m</i>)	R	Frequency (Hz)
1	5	0.05	0.5
2	10	0.05	0.5
3	5	0.05	0.5
4	10	0.05	0.5
5	5	0.05	0.5
6	10	0.05	0.5

The test matrix for the remaining laboratory-air tests will depend on the results of the preliminary testing. The variables which will be explored are the loading frequency, load magnitude, and temperature, but specific values will be based on the preliminary results.

3. SUMMARY AND FUTURE WORK

Characterizing the crack-growth behavior in Alloy 617 may provide useful input for a safety analysis of an Alloy 617 component subjected to fatigue loads. High-temperature crack-growth tests in air and in reactor-grade helium would provide data for establishing the crack-growth correlations in support of a ASME BPVC Section XI high-temperature flaw evaluation Code Case. This research has proposed crack-growth testing on Alloy 617 in regimes which have not previously been investigated. This includes temperatures up to 1000°C.

The crack-growth system at INL has been validated for testing in air by comparing the crack lengths computed by the DCPD to crack lengths measured from images of the specimen post-test. The crack length from both sources matched well with each other. The computed crack-growth rates also compared well with previous work using the same fatigue loading steps.

The next steps in this work will be to complete the laboratory-air testing discussed in Section 2.3. At the same time as the laboratory-air testing, an environmental control system will be revitalized on a second load frame. This will allow for crack-growth testing in an impure helium environment. The testing in the helium environment will apply the same fatigue loads and temperatures as the laboratory-air testing so that the environmental effect can be quantified, and the test results used in a Section XI high-temperature flaw evaluation Code Case.

4. References

- 1 ASME. (2021). Boiler and Pressure Vessel Code. New York, NY: ASME.
- 2 ASTM B168-19, Standard Specification for Nickel-Chromium-Iron Alloys (UNS N06600, N06601, N06603, N06690, N06693, N06025, N06045, and N06696) and Nickel-Chromium-Cobalt-Molybdenum Alloy (UNS N06617) Plate, Sheet, and Strip, PA: ASTM International.
- 3 Benz, J. and Wright R., Fatigue and Creep Crack Propagation behaviour of Alloy 617 in the Annealed and Aged Conditions, Third International Workshop on Structural Materials for Innovative Nuclear Systems, October 2013, INL/CON-13-30214.
- 4 Wright, R., Benz, J., Initial Results on Characterization of Elevated Temperature Crack Growth of Alloy 617. INL Engineering Calculation and Analysis Report, ECAR No. 1539, ECAR Rev. 0, Project File No. 23747, May 2011.

Page intentionally left blank

Appendix A
INL drawing 765572 Rev. 2.

